Water Research 88 (2016) 274–284

Contents lists available at ScienceDirect

Water Research

journal homepage: www.elsevier.com/locate/watres

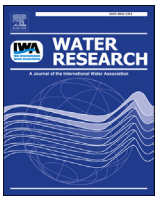

Critical role of surface roughness on colloid retention and release in porous media

Saeed Torkzaban [a, *], Scott A. Bradford [b]

[a] CSIRO Land and Water, Glen Osmond, SA 5064, Australia
[b] USDA, ARS, Salinity Laboratory, Riverside, CA 92507, United States

ARTICLE INFO

Article history:
Received 24 July 2015
Received in revised form
9 October 2015
Accepted 17 October 2015
Available online 19 October 2015

Keywords:
Colloid
Porous media
DLVO theory
Retention
Release

ABSTRACT

This paper examines the critical role of surface roughness (both nano- and micro-scale) on the processes of colloid retention and release in porous media under steady-state and transient chemical conditions. Nanoscale surface roughness (NSR) in the order of a few nanometers, which is common on natural solid surfaces, was incorporated into extended-DLVO calculations to quantify the magnitudes of interaction energy parameters (e.g. the energy barrier to attachment, $\Delta\Phi_a$, and detachment, $\Delta\Phi_d$, from a primary minimum). This information was subsequently used to explain the behavior of colloid retention and release in column and batch experiments under different ionic strength (IS) and pH conditions. Results demonstrated that the density and height of NSR significantly influenced the interaction energy parameters and consequently the extent and kinetics of colloid retention and release. In particular, values of $\Delta\Phi_a$ and $\Delta\Phi_d$ significantly decreased in the presence of NSR. Therefore, consistent with findings of column experiments, colloid retention in the primary minimum was predicted to occur at some specific locations on the sand surface, even at low IS conditions. However, NSR yielded a much weaker primary minimum interaction compared with that of smooth surfaces. Colloid release from primary minima upon decreasing IS and increasing pH was attributed to the impact of NSR on the values of $\Delta\Phi_d$. Pronounced differences in the amount of colloid retention in batch and column experiments indicated that primary minimum interactions were weak even at high IS conditions. Negligible colloid retention in batch experiments was attributed to hydrodynamic torques overcoming adhesive torques, whereas significant colloid retention in column experiments was attributed to nano- and micro-scale roughness which would dramatically alter the lever arms associated with hydrodynamic and adhesive torques.

1. Introduction

The processes of colloid (e.g., microbes, clays, and engineered nanoparticles) retention and release in porous media are of great importance in many environmental and industrial applications. For example, release and transport of in-situ clay particles during manage aquifer recharge and enhanced oil recovery may adversely affect the permeability of the near-well formation (Khilar and Fogler, 1998; Torkzaban et al., 2015). Surface water and wastewater treatment processes such as riverbank filtration, infiltration ponds and galleries, and sand filtration rely on the rate of retention and release of bio-colloids (viruses, bacteria, and protozoan parasites) during passage through porous media (Foppen and Schijven, 2006; Tufenkji et al., 2004; Knappett et al., 2008; Bradford et al., 2014). Therefore, a comprehensive understanding of factors that influence colloid retention to and release from solid surfaces is needed for the efficient design and successful operation of a wide variety of environmental and engineering processes.

Interaction energies between colloids and solid surfaces are commonly described as the sum of electrostatic double layer (EDL) and van der Waals (vdW) interactions using DLVO theory (Derjaguin and Landau, 1941; Verwey and Overbeek, 1948). Conditions are expected to be unfavorable for retention when the colloid and collector surfaces are like-charged and there exists a considerable repulsive energy barrier against the primary minimum interaction. However, one may create favorable conditions for retention in a primary or secondary energy minimum by altering the solution chemistry (e.g. lowering the pH or increasing the ionic strength) (Kuznar and Elimelech, 2007; Emelko, 2003; Jaisi and Elimelech, 2009; Liu et al., 2009). Classical DLVO theory predicts a

* Corresponding Author.
E-mail address: Saeed.Torkzaban@csiro.au (S. Torkzaban).

http://dx.doi.org/10.1016/j.watres.2015.10.022
0043-1354/

primary minimum of infinite depth, implying that the colloid would be in physical contact with the collector surface and therefore the likelihood of detachment by alteration of chemical conditions will be zero. However, the depth of the primary minimum is finite when DLVO theory is extended, commonly referred to as extended-DLVO, to include short-range repulsive interactions such as Born, Lewis acid–base, hydration, and steric interactions (Bergendahl and Grasso, 1999).

Numerous studies have pointed out the inadequacy of classical- and extended-DLVO calculations in explaining colloid retention and release in porous media (Bradford and Torkzaban, 2012; Tong et al., 2008; Tufenkji and Elimelech, 2005). For example, DLVO calculations predict the absence of a repulsive energy barrier and therefore primary minimum interaction when the solution ionic strength (IS) is high (e.g., >100 mM at a neutral pH). Under these conditions, the entire collector surface is expected to contribute (be available) to colloid retention. However, experimental evidence suggests that only a small fraction of the surface of porous media contributes to colloid retention under these "so-called" favorable conditions (Argent et al., 2015; Sasidharan et al., 2014; Magal et al., 2011; Treumann et al., 2014). Furthermore, mean-field DLVO theory, based on homogeneous surfaces of the colloid and collector, predicts when the IS is lowered to a few mM, the secondary minimum is completely eliminated and, as such, all of the colloids initially retained in the secondary minimum should be released. However, several studies have shown that only a fraction of the retained colloids was released when the secondary minimum was completely eliminated (Shen et al., 2012; Torkzaban et al., 2008, 2010). These findings suggest that a considerable fraction of colloids should have been retained in the primary minimum, even though the DLVO calculations predicted a high energy barrier against primary minimum attachment at the initial chemical conditions.

Extended-DLVO theory typically predicts the existence of a significant energy barrier against detachment from a primary minimum (e.g., >10 kT, where k is the Boltzmann constant and T is the absolute temperature), when the IS decreases to zero or the pH increases to alkaline conditions (Ryan and Elimelech, 1996). Brownian forces are therefore expected to produce negligible detachment due to the considerable energy barrier against detachment (Shen et al., 2012; Bradford and Torkzaban, 2013). In contrast, a substantial increase in the rate and extent of colloid release from the primary minimum has been experimentally observed when the IS and pH of the eluting solution was decreased and increased, respectively (e.g. Ryan and Gschwend, 1994; Bradford et al., 2015a, b). To explain this apparent contradiction, Ryan and Gschwend (1994) had to increase the Born collision parameter from 0.5 to 2 nm in their extended-DLVO calculations so that the energy profiles for retained colloids were repulsive. In another study, Bergendahl and Grasso (1999) studied the release of latex colloids from primary minima by increasing the solution pH in packed-bed columns. A portion of the retained colloids was found to release with each stepwise increase in pH. In contrast, extended-DLVO theory predicted complete colloid detachment when the pH increased above a threshold value.

Conventional DLVO calculations consider that interacting surfaces are perfectly smooth. However, natural solid surfaces (e.g., sand grains) always contain some degree of surface roughness (Darbha et al., 2012; Morales et al., 2009). For example, atomic force microscopy (AFM) analysis of glass bead and sand surfaces showed a wide range of roughness varying from a few nanometers up to several hundreds of micrometers (Shellenberger and Logan, 2002; Shen et al., 2011; Konopinski et al., 2012). The impact of nanoscale surface roughness (NSR) on interaction energy profiles has been investigated in several studies (Suresh and Walz, 1996; Bendersky and Davis, 2011; Hoek and Agarwal, 2006; Bhattacharjee et al., 1998; Huang et al., 2010; Shen et al., 2011). NSR has been shown to reduce the magnitude of the secondary minimum and may locally reduce and/or eliminate the energy barrier to the primary minimum under macroscopically unfavorable conditions (Huang et al., 2010; Shen et al., 2011). In addition, extended-DLVO calculations have indicated that the depth of the primary minimum was considerably shallower on rough than on smooth surfaces (Bradford and Torkzaban, 2013; Shen et al., 2012). NSR may therefore provide a plausible explanation for observed hydrodynamic removal of colloids in batch systems under favorable conditions (Treumann et al., 2014), but no studies have yet been conducted to rigorously test this hypothesis. The situation is more complex in column studies because nano- and microscale roughness may also dramatically alter the lever arms associated with the applied hydrodynamic and resisting adhesive torques (Bradford et al., 2013). Indeed, enhanced colloid retention has been observed to occur at locations associated with microscale roughness and grain–grain contacts under unfavorable attachment conditions (Darbha et al., 2012; Torkzaban et al., 2008). This behavior has commonly been attributed to secondary minimum retention (Torkzaban et al., 2008), even though incomplete recovery of colloids in the presence of deionized water suggests that primary minimum retention played an important role. To date, no systematic theoretical and experimental studies have been conducted to investigate the role of NSR on colloid retention to and release from a primary energy minimum in column and batch systems.

The overall objective of this study was to reveal the critical role of surface roughness (both nano- and micro-scale) on the processes of colloid retention and release in porous media under steady-state and transient chemical conditions. This aim was achieved by first theoretically investigating the effects of NSR on interaction energy parameters, namely, secondary and primary minima, and the energy barrier to attachment and detachment from a primary minimum. We then present results of a series of batch and column experiments that were conducted by employing ultrapure quartz sand and two colloid sizes (0.5 and 2 μm) at various solution IS and pH conditions. Batch experiments were conducted to minimize the effect of surface roughness (especially microscale asperities) on effective lever arms and corresponding hydrodynamic and adhesive torques and to experimentally demonstrate the influence of NSR on the interaction energies and colloid retention process. We employed ultrapure quartz sand and carboxylate-modified latex particles as models for porous media and colloids, respectively, in order to minimize the effect of chemical heterogeneities on our results.

2. Materials and methods

2.1. Colloids, sand, and electrolyte solutions

Two different sizes (0.5 and 2 μm) of carboxylate-modified latex (CML) particles (Invitrogen, Inc.) were used as model colloids in batch and column experiments. Ultrapure quartz sand (Unimin Corp. NC) was employed as the porous medium in the experiments. Further details on the colloids, analysis, concentrations, and sand properties are given in the Supporting materials (SM) Section S1. Electrolyte solutions were prepared using Milli-Q water (pH = 5.8) and NaCl with the IS ranging from 0 to 800 mM. When required, the pH of the solution was increased to 10 by addition of NaOH (1 mM).

2.2. Colloid size and zeta potentials measurements

The hydrodynamic diameter of the colloids in various electrolyte solutions was assessed using a Zetasizer (Malvern Instruments, USA). The manufacturer reported that the CML colloids are stable in concentrations of electrolyte up to 1 M univalent salt. We also

confirmed that the colloid suspension was stable over the time span of batch and column experiments and did not observe any aggregation, even at the highest tested IS of 0.8 M. The zeta potential of the colloids and crushed quartz sand in various experimental solutions was determined from measured electrophoretic mobilities using the Zetasizer and the Smoluchowski equation. The measurements were repeated five times for each colloid suspension. A summary of the zeta potential measurements is presented in Table S1.

2.3. Interaction energy on homogeneous surfaces

Extended-DLVO theory was used to calculate the total interaction energy (Φ) of colloids upon close approach to a perfectly smooth and chemically homogeneous sand surface in various experimental solutions. In these calculations, retarded London-van der Waals (vdW) attractive interaction was determined from the expression of Gregory (Gregory, 1981) utilizing a value of 1.0×10^{-20} J for the Hamaker constant to represent the latex–water–quartz system (Elimelech and O'Melia, 1990). Electrostatic double layer (EDL) interaction was quantified using the expression of Hogg et al. (1966), with zeta potentials in place of surface potentials. Short-range repulsive interactions dominate Φ at very short separation distances. Ruckenstein and Prieve (1976) used the repulsive term of the interatomic Lennard-Jones m-n potential to derive an expression for the Born repulsion that was used in this study. The collision diameter was set equal to 0.26 nm to achieve a primary minimum depth at 0.157 nm, a commonly accepted distance of closest approach (van Oss, 1994). Other short-range repulsive interactions (e.g., steric, hydrophobic, solvation, hydrogen bonding, and Lewis acid–base forces) were not considered in our analysis because their origins and relevant parameters are still poorly understood. For completeness, the equations used in the extended-DLVO calculations are given in the SM Section S2.

2.4. Interaction energy on nanoscale rough surfaces

Natural solid surfaces (e.g., glass beads and sand grains) always exhibit wide distributions of roughness height, shape, and size (Shellenberger and Logan, 2002; Shen et al., 2011; Konopinski et al., 2012). For example, Shen et al. (2011) using AFM analysis showed that the average and maximum roughness for sand was 293 and 2418 nm, respectively. These values were 80 and 627 nm, respectively, even for smooth glass bead surfaces (Shellenberger and Logan, 2002). Experimental determination of these roughness parameters on the natural surfaces (e.g., via AFM) is a daunting task, and generation of spatial maps of explicit roughness properties is not practical, so simplified random representations are typically considered. Similar to Bendersky and Davis (2011), NSR is represented in this work as nanoscale pillars with given height (h_r) and density that are randomly distributed on over the collector (sand) surface. It is further assumed that the cross sectional area of each pillar is much smaller than the size of the zone of electrostatic influence (A_z) and that the nanoscale roughness is directly below the colloid (Bendersky and Davis, 2011). In this case, the mean value of the total interaction energy can be determined by a linear combination of the interaction energy associated with the asperity tops and the underlying smooth surface as (Bendersky and Davis, 2011; Bradford and Torkzaban, 2013):

$$\Phi(h) = (1-f)\Phi(h+h_r) + f\Phi(h) \quad [1]$$

where h is the distance of closest approach between the colloid and the asperity top, and f is the roughness density in A_z having a fixed roughness height of h_r. In an attempt to represent wide distributions of roughness height and density on sand surfaces, we assumed that values of h_r and f range from 0 to 50 nm and 0.5–10%, respectively. Note that Eq. [1] is consistent with results from surface integration techniques reported in the literature (Huang et al., 2010; Shen et al., 2012). Specifically, Huang et al. (2010) demonstrated through surface element integration technique that Eq. [1] can be used to assess the influence of NSR on Φ over a wide range of roughness morphologies, provided the colloid radius is considerably larger than the roughness size. This condition is obviously satisfied in our study in which the ratio of colloid radius to roughness height was always greater than 5. The applicability of this simple equation to examine the influence of NSR, when the Born repulsion was included in the interaction energy calculations, was recently confirmed by comparison of results from grid surface integration simulations (Bradford and Torkzaban, 2013).

2.5. Batch experiments

A series of batch experiments was conducted by placing 31 g of sand and 31 mL of a colloid suspension into 42 mL glass tubes. To provide complete mixing, the tubes were rotated on a 90° angle with a tube rotator at a speed of 10 rpm. Various solution IS were considered in the experiments, as indicated in Table S1. The tubes were agitated for another 2 h during which the aqueous colloid concentration was measured at several intervals. This cycle was continued until little decrease (<5%) in the colloid concentration was observed over the course of 2 h. Following the completion of the batch experiments, scanning electron microscopy (SEM) was performed on several sand grains to visualize the distribution of attached colloids on sand surfaces. Details of the batch experiments and SEM imaging are given in the SM Sections S3 and S4, respectively.

The decrease in the aqueous colloid concentration with time was attributed to net irreversible attachment to the sand surfaces, as was demonstrated in our previous study (Treumann et al., 2014). The difference in the final and initial colloid concentration in each cycle of the batch experiment was summed and used to calculate the maximum colloid concentration on the sand surface (S_{max}) at any given IS. The maximum fraction of the sand surface that contributed to colloid retention (S_f) at any given IS was determined using the following equation (Bradford et al., 2012):

$$S_f = \frac{A_c \rho_b S_{max}}{(1-\gamma)A_s} \quad [2]$$

where A_c [L^2 N_c^{-1}] is the cross section area per colloid, A_s [L^{-1}] is the solid surface (sand) area per unit volume, ρ_b[ML^{-3}] is the sand bulk density, and γ [-] is the porosity of a monolayer packing of colloids on the solid surface. The value of γ was set equal to 0.5 based on information presented by Johnson and Elimelech (1995). Eq. [2]is valid for monolayer coverage of colloids on the collector surface. This assumption was confirmed by visual inspection of the SEM images, presented in the SM (Fig. S1).

2.6. Torque balance analysis of batch experiments

A torque balance analysis was conducted to examine the mechanism of colloid attachment to sand surfaces in the batch experiments. Relevant adhesive and hydrodynamic forces, lever arms, and torques which act on a colloid adjacent to the sand surface were calculated. Colloid retention on a solid surface is controlled by the balance of applied hydrodynamic (T_A) and resisting adhesive torques (T_H), when the strength of the

interaction energy (primary or secondary minimum) is greater than the colloid thermal energy (e.g., a few kT) (Bradford et al., 2013). In this case, attachment occurs when $T_A \geq T_H$. Full details of the torque balance calculations are given in the SM Section S5.

2.7. Column experiments

Column experiments were performed using acrylic columns with a length of 11 cm and a radius of 1 cm. The columns were wet packed with the ultrapure quartz sand. The porosity was calculated gravimetrically to be about 0.4, and the volume associated with one pore volume (PV) was 13.8 cm^3. A syringe pump was used to pump the solutions into the column at a constant average pore water velocity (v) of 5 m/d. The flow direction was vertically upward. Note that the potential effect of gravity force on the kinetics of colloid retention and release was not considered in the present study. This effect has been shown to be important for colloid transport, especially for larger and denser particles (Chrysikopoulos and Syngouna, 2014). A fraction collector was used to continuously collect the effluent samples. Colloid retention was assessed by injection of a pulse of colloid suspension (at various IS and pH = 5.8) into the column for several PVs (phase 1), followed by a colloid-free solution of the same chemistry for several additional PVs (phase 2). Colloid release and the reversibility of colloid retention was investigated with a step reduction of solution IS to that of DI water at pH 5.8 (phase 3), followed by injection of several PVs of DI water at pH 10 (phase 4). Following the completion of column experiments, the sand was excavated from the column and placed in a container containing excess amounts of DI water at pH adjusted to 10. The container was slowly shaken for several minutes to investigate the release of any remaining retained colloids. The colloid concentration in the excess water was measured and the volume of water and mass of dry sand was determined.

Colloid transport experiments were conducted in duplicate at each solution IS. The colloid mass recovery (%) was calculated as the ratio of the mass of released colloids during each release phase to the mass of retained colloids during phase 1 and 2. Table S2 provides a summary of parameters and mass balance information of the column experiments.

3. Results and discussion

3.1. Interaction energy on smooth surfaces

Table S1 lists the values of zeta potentials of the CML colloids and quartz sands over a wide range of solution chemistries. We observe that the colloids and sand surfaces become less negatively charged with increasing IS. In addition, an increase in pH from 5.8 to 10 caused the surfaces of colloids and quartz to become more negatively changed, indicating further deprotonation of the surfaces. We used these measured zeta potentials to calculate interaction energy parameters, namely, the depth of secondary energy minimum ($\Phi_{2^0\min}$), the energy barrier height ($\Phi_{\max}$), the depth of primary energy minimum ($\Phi_{1^0\min}$), the energy barrier to attachment in the primary minimum ($\Delta\Phi_a = \Phi_{\max} - \Phi_{2^0\min}$), and the energy barrier to detachment from the primary minimum ($\Delta\Phi_d = \Phi_{\max} - \Phi_{1^0\min}$) for the colloid-quartz systems. Values of these parameters at the different solution chemistries are listed in Table S1. As expected, the extended-DLVO calculations, by treating the sand surface as being perfectly smooth, revealed very small values of $\Phi_{2^0\min}$ when IS < 30 mM. Hence, we expect negligible colloid retention in the secondary minimum when IS < 30 mM. In contrast, we note that the magnitude of $\Phi_{2^0\min}$ increased with IS and colloid size; for example 2.9 kT for the 0.5 μm colloid and 10 kT for the 2 μm colloid at 30 mM. Thus, we speculate that colloid retention on the sand surface would occur via the secondary minimum when the IS ≥ 30 mM, provided that $T_A \geq T_H$ (Bradford et al., 2013). However, a complete and rapid release of the colloids should occur upon lowering the IS to ca. 10 mM, since the value of $\Phi_{2^0\min}$ becomes negligible when the IS approaches to zero (see Table S1).

In Table S1, we observe very high values of $\Delta\Phi_a$ for both colloids when IS ≤ 50 mM (>106 kT for 2 μm colloid and >22 kT for 0.5 μm colloid). Therefore, it is unlikely to have colloid attachment in the primary minimum under these conditions, that is, smooth surfaces and IS ≤ 50 mM. Conversely, the value of $\Delta\Phi_a$ became zero and a very high value of $\Phi_{1^0\min}$ (i.e. a very deep primary energy minimum) was calculated for the colloids when IS ≥ 100 mM. Therefore, the colloids are expected to strongly attach onto the sand surface, if it was indeed perfectly smooth, in a primary energy minimum when IS ≥ 100 mM. Thus, the entire sand surface should be available for colloid retention (i.e. $S_f = 1$). Furthermore, when colloids are attached into the primary minimum at these conditions, their release (detachment) is very unlikely even if the IS is lowered to 0.1 mM. This is because the values of $\Delta\Phi_d$ remained very high (>3000 kT for 2 μm and >700 kT for 0.5 μm at IS of 0.1 mM). Similarly, negligible release for colloids initially attached in the primary minimum at IS > 100 mM is expected upon increasing the pH to 10. This result is indeed expected, since DLVO calculations indicate that the vdW attraction dominates the repulsive interactions as separation distances associated with the primary minimum.

3.2. Interaction energy on nanoscale rough surfaces

3.2.1. Influence of NSR on secondary energy minimum

Fig. 1 presents magnitudes of $\Phi_{2^0\min}$ as a function of h_r and f for the 2 and 0.5 μm colloids when the IS was 30 and 50 mM NaCl. We note that an increase in h_r significantly decreased the magnitude of $\Phi_{2^0\min}$ at a given value of f and IS. For example, the value of $\Phi_{2^0\min}$ for the 2 μm colloid at IS of 50 mM decreased from 22 kT for a perfectly smooth collector surface to less than 5 kT when $h_r \geq 20$ nm (Fig. 1c). This decrease of $\Phi_{2^0\min}$ is attributed to the reduced contribution of the vdW attraction in the presence of roughness. Thus, we expect that secondary minimum retention of colloids on rough surfaces is more vulnerable to detachment by Brownian and hydrodynamic forces than that of smooth surfaces. Hence, NSR is predicted to considerably reduce the amount of colloid retention on solid surfaces via a secondary energy minimum. This finding is in agreement with previous theoretical and experimental studies that have demonstrated that NSR greatly reduces the magnitude of $\Phi_{2^0\min}$ (Huang et al., 2010; Bhattacharjee et al., 1998). In comparison to h_r, we found that nanoscale roughness density (the value of f) had little effect on the value of $\Phi_{2^0\min}$ over the examined parameter ranges (see Fig. 1).

3.2.2. Influence of NSR on the energy barrier to attachment in the primary minimum

Fig. 2 shows that NSR significantly reduced the magnitudes of $\Delta\Phi_a$ in comparison to a smooth surface ($h_r = 0$) when IS = 10 and 50 mM. For example, the value of $\Delta\Phi_a$ for the 2 μm colloid at IS of 10 mM decreased from 680 kT on a smooth surface to less than 10 kT when $h_r > 15$ nm and f<3%. The reduction in $\Delta\Phi_a$ was even more pronounced for the 0.5 μm colloid. The influence of h_r and f on $\Delta\Phi_a$ was greater when the IS was increased from 10 mM to 50 mM (see Fig. 2c and d). When the IS = 50 mM, the value of $\Delta\Phi_a$ completely disappeared at some locations associated with certain combinations of f and h_r. Fig. 2c and d shows that the value of $\Delta\Phi_a$ increased with further increase of h_r at a given value of f. This is due to different relationships for EDL and vdW interactions with

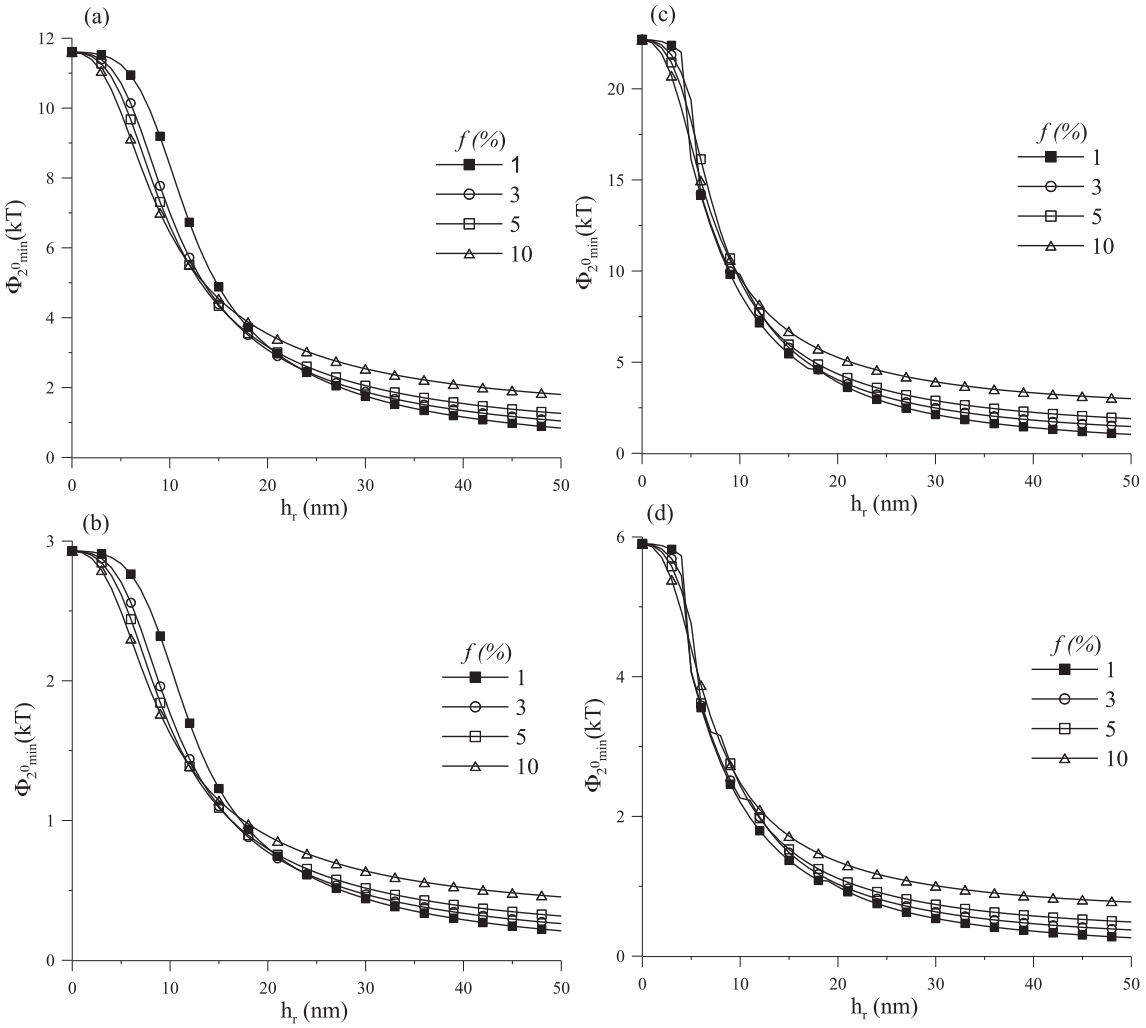

Fig. 1. Calculated values of the secondary minimum depth ($\Phi_{2^0\min}$) as a function of roughness height (h_r) for various roughness densities, f, (1, 3, 5, and 10%) at IS = 30 mM in (a & b) and 50 mM in (c & d). The colloid size was 2 μm in (a & c) and 0.5 μm in (b & d). The zeta potential values used in the calculations are given in Table S1. Note the change in scale of the y axis in the graphs.

separation distance. The Maxwellian kinetic energy model predicts a rapid increase in the probability of colloids to overcome an energy barrier as the value of $\Delta\Phi_a$ decreases to less than 10 kT (Simoni et al., 1998; Bradford et al., 2012). Therefore, these results indicate that primary minimum attachment is plausible at some locations on the sand surface associated with a specific combination of f and h_r. This effect of NSR on $\Delta\Phi_a$ is consistent with the findings of previous studies reported in the literature (Hoek and Agarwal, 2006; Henry et al., 2011; Chen et al., 2010).

3.2.3. *Influence of NSR on primary energy minimum*

Fig. 3 shows that the presence of NSR significantly reduced the magnitude of $\Phi_{1^0\min}$ in comparison to a smooth surface when IS = 100 mM, 300 mM (for the 0.5 μm colloid), and 500 mM (for the 2 μm colloid). The maximum depth of $\Phi_{1^0\min}$ occurred on a smooth surface (h_r = 0). Increasing h_r and decreasing f significantly decreased the value of $\Phi_{1^0\min}$ due to the reduced contribution of the attractive vdW interaction in the presence of NSR. For example, values of $\Phi_{1^0\min}$ were reduced to smaller than 20 kT for the 0.5 μm colloid when h_r > 5 nm and f<5%. The strength of colloid retention in the primary minimum should therefore be much weaker at rough compared to smooth surfaces. These results are in agreement with the AFM measurements reported in the literature (Bowen and Doneva, 2000; Katainen et al., 2006) and with theoretical calculations (Shen et al., 2012; Argent et al., 2015). Consequently, primary minimum attachment of colloids at a rough location on the sand surface is expected to behave in many ways like those in the secondary minimum. We can speculate that colloid retention in a shallow $\Phi_{1^0\min}$ is vulnerable to detachment by hydrodynamic shear forces.

3.2.4. *Influence of NSR on the energy barrier against detachment from the primary minimum ($\Delta\Phi_d$)*

Fig. 4 presents values of $\Delta\Phi_d$ as a function of h_r and f for the 0.5 and 2 μm colloids when IS = 0.1 mM and pH = 5.8 and 10. For a given value of f, values of $\Delta\Phi_d$ initially decreased dramatically with increasing h_r due to the reduced contribution of vdW interaction. However, further increases in h_r resulted in an increase in the value of $\Delta\Phi_d$ due to the different dependencies of the vdW and EDL interactions on h_r that yielded a greater reduction in the repulsive EDL interaction. Nevertheless, the value of $\Delta\Phi_d$ was still considerably lower on a rough than a smooth surface. For example, the value of $\Delta\Phi_d$ for 2 μm colloids decreased from 3502 kT for a perfectly smooth surface to less than 10 kT when $f \leq$ 1% and h_r > 7 nm (Fig. 4a), and completely disappeared when $f \leq$ 0.5% and h_r > 7 nm. These same general trends were observed for the 0.5 μm colloid in Fig. 4b, but $\Delta\Phi_d$ was reduced or eliminated over a greater range of f and h_r in comparison with 2 μm colloids. Hence, colloid release

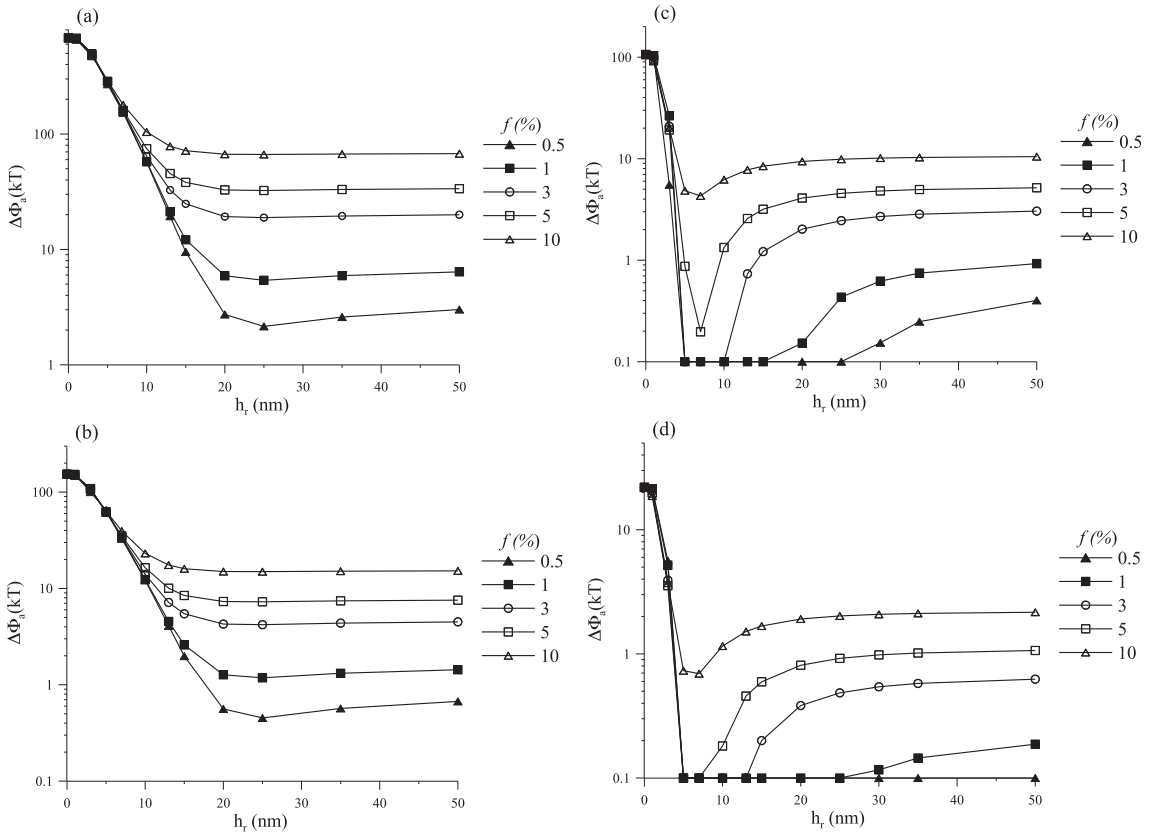

Fig. 2. Calculated values of the energy barrier to attachment in the primary energy minimum ($\Delta\Phi_a = \Phi_{max} - \Phi_{2^0min}$) as a function of roughness height (h_r) for various roughness densities, *f*, (0.5, 1, 2, 3, 5, and 10%) at IS = 10 mM in (a & b) and 50 mM in (c & d). The colloid size was 2 μm in (a & c) and 0.5 μm in (b & d). Note the change in scale of the *y* axis in the graphs.

from primary minimum may occur upon reducing the IS to 0.1 mM if they were located atop specific rough spots (e.g. f = 1% and h_r~15 nm); whereas some would still remain attached depending on the roughness properties of their A_z (e.g. f >3%). Furthermore, Fig. 4c and d reveal that $\Delta\Phi_d$ was further reduced over a wider range of f and h_r when pH increased from 5.8 to 10, suggesting that an additional amount of colloid release from the primary minimum may occur with an increase in pH.

It is worthwhile mentioning that the above values of $\Delta\Phi_d$ and also Φ_{1^0min} should be regarded as semi-qualitative because of the various assumptions used in the interaction energy calculations. Nevertheless, our results clearly demonstrate enormous changes in the interaction energy parameters in the presence of NSR. Thus, we tend to believe that the correct trends were captured by our simplified description of surface roughness.

3.3. Batch experiments

Fig. 5 presents representative plots of the normalized colloid concentrations (C/C_i; where C_i is the initial colloid concentration) as a function of time in the batch experiments for various solution IS. Negligible colloid attachment to the sand surfaces was observed for the 2 and 0.5 μm colloids when the IS was less than 100 and 20 mM, respectively (data not shown). These findings confirmed the absence of significant amounts of chemical heterogeneities such as micro- or macro-scale positively-charged metal oxides on the quartz surfaces. Indeed, we chose to conduct the laboratory experiment using ultra-pure quartz sand in order to minimize the effect of chemical heterogeneities on our results. We observed that when IS ≥ 100 mM for the 2 μm colloids and ≥30 mM for the 0.5 μm colloids, the value of C/C_i began to decrease with time, indicating colloid attachment onto the sand surfaces. In order to determine the maximum attainable colloid concentration on the sand surface (S_{max}), we replaced the excess colloid suspension after the 2 h of mixing with a new colloid suspension and the batch tubes were agitated for another 2 h. This cycle was continued until the aqueous colloid concentration decreased very little (<5%) over the course of 2 h of agitation. We therefore confirmed that all of the attachment sites on the sand surfaces were filled with the colloids. It should be noted that the colloid suspension over the range of solution IS (up to 0.8 M) was confirmed to be stable using the Zetasizer and controlled tubes containing no sand. We also confirmed that colloid attachment to the sand surfaces was irreversible (see Section 2.5) in agreement with our previous study (Treumann et al., 2014). Furthermore, SEM images, shown in Fig. S1, also confirmed the presence of monolayer colloid attachment on the sand surfaces, ruling out any potential effect of aggregation and ripening in our experiments even at the highest tested IS (0.8 M).

Values of S_f for each colloid size and solution IS were calculated using Eq. [2] based on the measured values of S_{max} obtained after several cycles of the batch experiments. We found the values of S_f to be very small (<1%), even when the IS was as high as 800 and 300 mM for the 2 and 0.5 μm colloids, respectively (see Table S3). These findings revealed that only a very small fraction of the sand surface contributed to colloid retention in the batch experiments. Note that extended-DLVO calculations for a smooth collector surface predicted the presence of a very deep primary energy minimum when IS ≥ 100 mM (see Table S1), suggesting that the entire sand surface should have been available for attachment (i.e. S_f = 100%). In contrast, the small S_f values clearly demonstrate that the strength of primary energy minimum over the majority of the sand surfaces was not strong enough to produce attachment, even

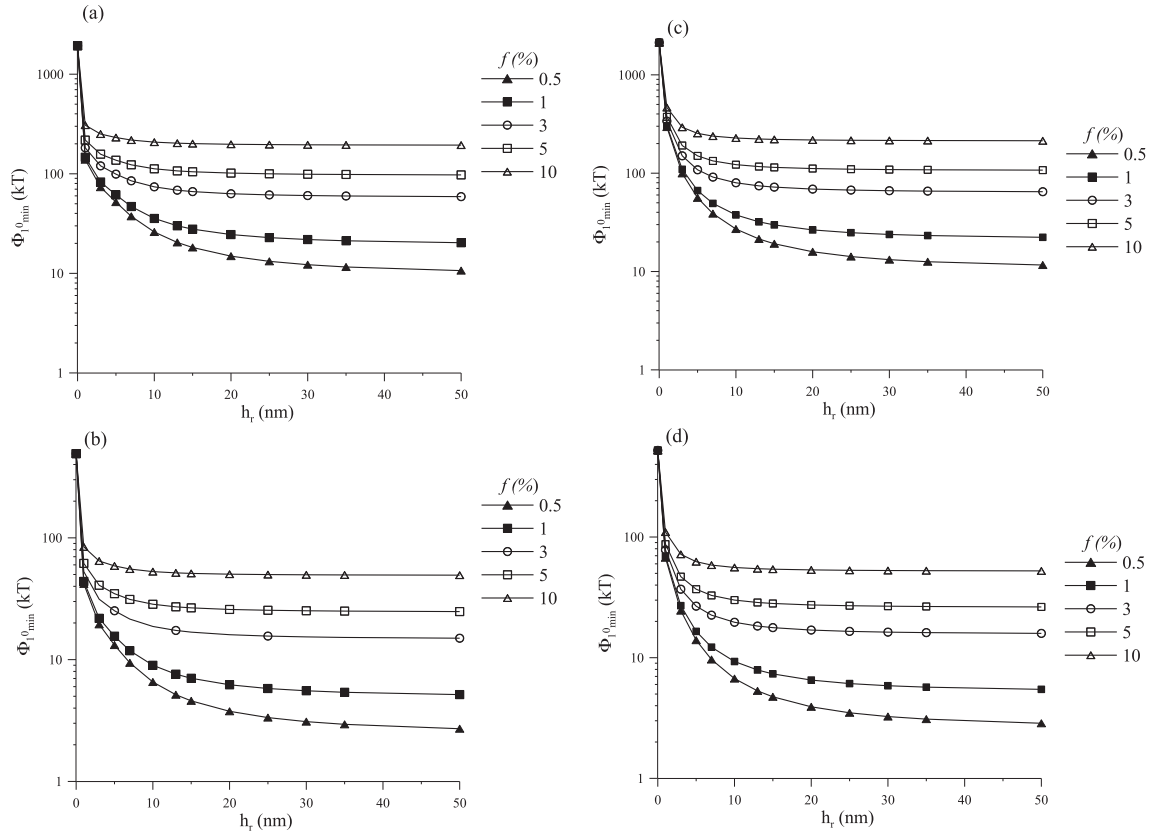

Fig. 3. Calculated values of the primary minimum depth ($\Phi_{1^{o}min}$) as a function of roughness height (h_r) for various roughness densities, *f*, (0.5, 1, 2, 3, 5, and 10%) at IS = 100 mM in (a & b) and 500 mM in (c) and 300 mM in (d). The colloid size was 2 μm in (a & c) and 0.5 μm in (b & d).

at the IS of 800 mM. It is obvious that the gentle agitation (note that the speed the tube rotator was set at the minimum of 10 rpm) during the batch experiments produced hydrodynamic shear forces that were sufficient to prevent colloid attachment over the majority of the sand surfaces.

3.4. Torque balance calculations for batch experiments

The flow regime was found to be laminar in the batch tubes as the Reynolds number was determined to be very small ($Re<<1$), and the shear rate was estimated (Eq. [S5]) to be 35 s^{-1}. The value of hydrodynamic applied torque acting on the colloid adjacent to the sand surface was calculated (Eq. [S8]) to be 1.6×10^{-18} and 2.5×10^{-20} (N m^{-1}) for the 2 and 0.5 μm colloids, respectively. Based on the values of $\Phi_{1^{o}min}$ for a smooth surface at 100 mM (see Table S1) and using the JKR adhesion model, values of adhesive torque for the 2 and 0.5 μm were estimated (Eqs. [S9]-[S10]) to be 5.0×10^{-16} and 5.38×10^{-17} (N m^{-1}), respectively. We observe that the values of T_A were always larger than those of T_H (by several orders of magnitudes) for both colloids when the IS was ≥100 mM. Hence, colloid attachment should have occurred over the entire surface (i.e. $S_f = 1$) when IS > 100 mM if the sand surface was perfectly smooth. The torque balance analysis, however, did not consider the potential influence of NSR on the adhesive interaction energies and the lever arms associated with T_A and T_H. We already observed in Fig. 3 that NSR may significantly reduce the value of Φ_{1min}. Thus, we concluded that NSR and hydrodynamic shear forces provide a viable explanation for the observed very small amount of colloid attachment in the batch experiments. It should be mentioned that SEM images visually confirmed the small number of attached colloids (see Fig. S1). In addition, we observed that colloid attachment mainly occurred on microscale rough locations composed of ridges and valleys because of the negligible hydrodynamic forces associated with these regions (Treumann et al., 2014).

3.5. Column experiments

Fig. 6 presents representative normalized breakthrough concentrations (BTCs) of the 2 and 0.5 μm colloids for various IS values. In this case, C/C_0 (where C_0 is the influent colloid concentration) values were plotted as a function of pore volumes. We observed that colloid retention increased dramatically with increasing IS. Notably, more than 90% of the injected colloids were retained in the column when the IS was 100 mM. We found negligible colloid retention when the IS was 0.1 mM during phases 1 and 2 (data not shown). Thus, we concluded that physical entrapment of the colloids in small pore throats or wedges did not occur in our column experiments. These results are consistent with previous column studies for various colloids and porous media (Syngouna and Chrysikopoulos, 2011; Tosco et al., 2009; Shang et al., 2013).

We believe the significant difference between our column and batch results can be explained by torque balance considerations. Micro- and nano-scale surface roughness is known to greatly influence the lever arms that are associated with T_A and T_H (Bradford et al., 2013). In particular, when a colloid rests against a vertical protrusion, the lever arm for T_H and T_A is dramatically decreased and increased, respectively. For example, a simple trigonometry calculation indicates that even a 10 nm asperity can provide an effective lever arm for T_A that is orders of magnitude greater than the corresponding lever arm estimated for a smooth surface (Bradford et al., 2013). Colloid retention is therefore expected to

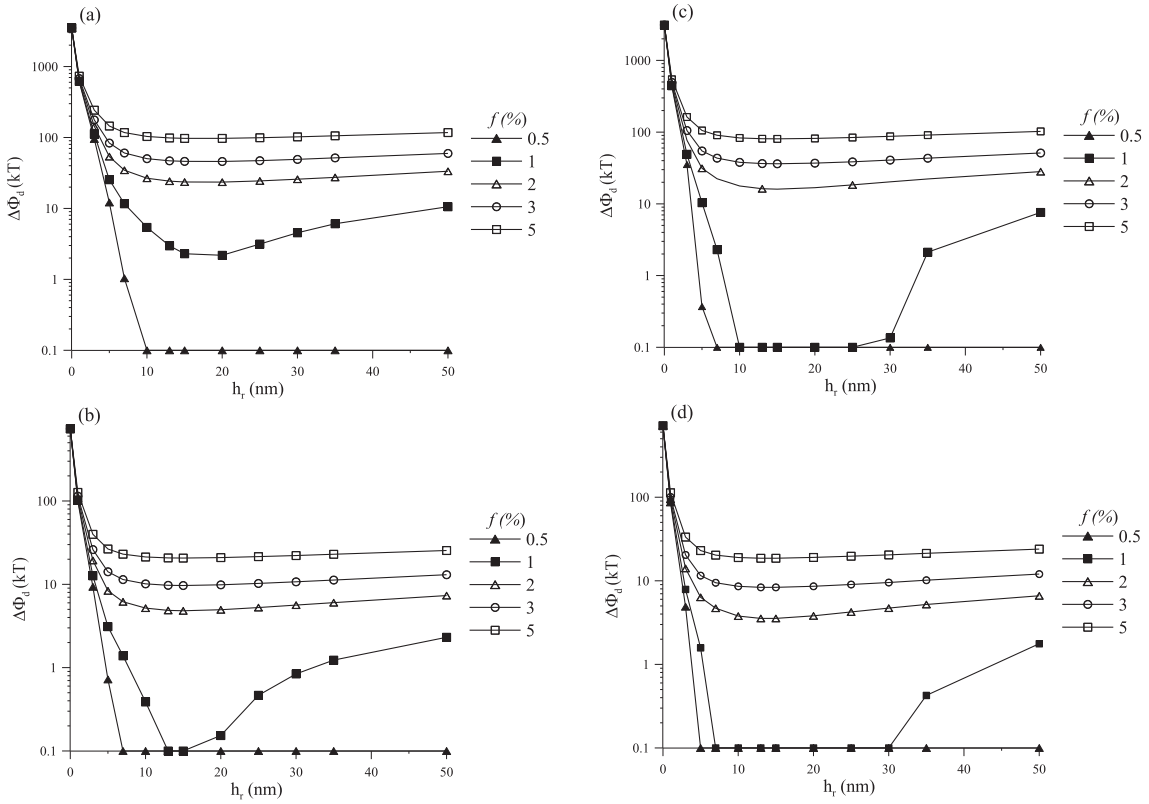

Fig. 4. Calculated values of the energy barrier to detachment from the primary minimum ($\Delta\Phi_d = \Phi_{max} - \Phi_{1^0min}$) as a function of roughness height (h_r) for various roughness densities, f, (0.5, 1, 2, 3, 5, and 10%) at IS = 0.1 mM and pH = 5.8 in (a & b) and pH 10 (c & d). The colloid size was 2 μm in (a & c) and 0.5 μm in (b & d)). Note the change in scale of the y axis in the graphs.

predominantly occur at locations associated with large scale roughness and ridges and valleys on sand grains when T_A is greater than T_H. In batch experiments, the direction and magnitude of T_H and T_A at a particular location on the grain surface are continuously altered with time. Thus, the torque balance criterion is not satisfied in a batch system. In contrast, the direction and magnitude of T_H and T_A are constant at a particular location on the sand surface in the static column system under steady-state conditions. Consequently, the negligible colloid attachment in our batch experiments and the significant retention in the column experiments under tested IS conditions demonstrate the importance of microscale surface roughness on colloid retention in porous media.

Fig. 6 also shows colloid release behavior when the IS was reduced to that of DI water at pH 5.8 (phase 3) and when the pH was increased to 10 (phase 4). The mass recovery in each phase is given in Table S2 for each colloid size and solution chemistry. The step decrease in IS to that of DI water resulted in a sudden and pulse-like release of retained colloids within the first and second PVs which gradually decreased with time. Another considerable fraction of the remaining colloids was released when the pH was increased to 10 (phase 4). Mass balance calculations revealed that a fraction of the retained colloids (3–80% and 20–40% for the 2 and 0.5 μm colloids, respectively) was not recovered even after flushing the column with DI water at pH 10. However, all of the remaining colloids were recovered when the sand was excavated from the column and placed in a container containing DI water at pH 10 and gently shaken for a few minutes (Table S2). In general, the 2 μm colloids were more reversibly retained than the 0.5 μm colloids when the IS of the retention phase (phase 1) was low, whereas the opposite trend was observed when IS was higher. It is worth mentioning that one might be tempted to attribute the colloid release in phase 4 to the presence of nanoscale chemical heterogeneities (NCH) on the sand surface. This is motivated by the fact that the charge of most metal oxides reverses from a positive to a negative value as the pH is increased to 10. However, in the absence of NSR, charge reversal of chemical heterogeneities would be unlikely to result in colloid release from a primary minimum during phase 4, since vdW attraction exceeds EDL repulsion at separation distance associated with the primary minimum in the absence of NSR. Indeed, Shen et al. (2013) theoretically demonstrated that colloid retention on chemical heterogeneity is irreversible upon perturbations in solution chemistry.

The observed extent and rate of colloid retention and release in the column experiments are not consistent with predictions of extended-DLVO theory on smooth surfaces. We observed that only a fraction of retained colloids was released following DI water elution during phase 3. This finding indicates that a substantial amount, if not all, of the retained colloids was interacting in the primary minimum even at the low IS of 10 mM. Similar to the batch experiments, the complete recovery of the colloids following sand excavation imply that the strength of primary minimum interaction was not large enough to overcome the hydrodynamic shear forces. These observations suggest that the retained colloids were held in shallow primary minima that was susceptible to hydrodynamic removal when the lever arms were altered.

NSR provides a viable explanation for the observed behavior of colloid retention and release in the column experiments. In particular, incorporating NSR into the extended-DLVO calculations demonstrated that primary-minimum colloid attachment is plausible even at low values of IS. NSR is ubiquitous on all natural solid surfaces. Hence, we conclude that NSR plays a key role in facilitating significant colloid retention under "so-called" unfavorable conditions which have been commonly observed (Tufenkji et al., 2004; Torkzaban et al., 2010). Interestingly, NSR can also provide

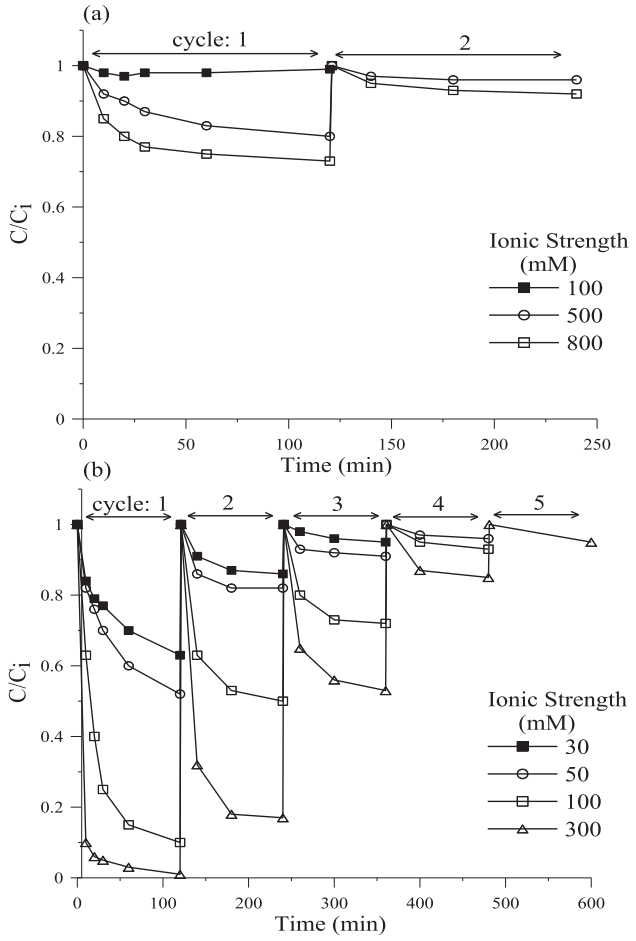

Fig. 5. Normalized colloid concentrations (C/C_i: where C_i is the initial colloid concentration) as a function of time for various values of IS in the batch experiments. Note the colloid suspension in the batch tube was replaced with a new solution of the same C_i at the end of each cycle. The colloid size was 2 μm in (a) and 0.5 μm in (b).

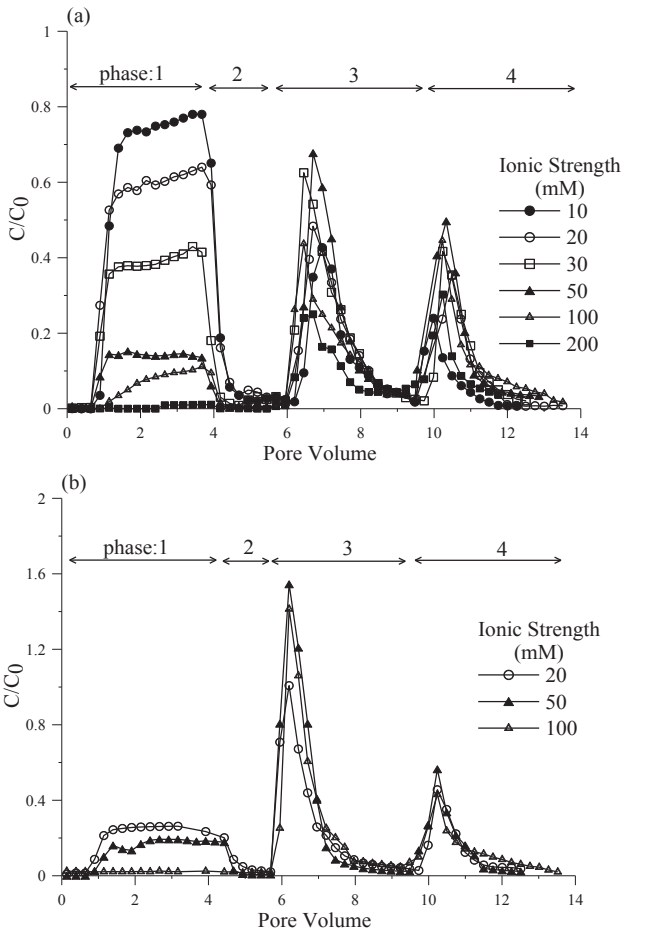

Fig. 6. Normalized effluent colloid concentrations (C/C_0: where C_0 is the influent colloid concentration) as a function of pore volume for various column experiments when the average pore water velocity was 5 m/day. The colloid size was 2 μm in (a) and 0.5 μm in (b). The sequence of the experiments was as follow: Phase 1: deposition of colloids in the column at various IS indicated in the legend; Phase 2: elution with the colloid-free solution of the same IS; Phase 3: elution with DI water; Phase 4: elusion with DI water at pH 10. Note the pH of the solutions in phase 1 to 3 was 5.8. Other experimental conditions are summarized in Table S2.

a sound explanation for the fractional colloid release upon perturbations in solution chemistry (Fig. 6). NSR may reduce or eliminate $\Delta\Phi_d$ to levels that colloids may overcome the energy barrier via their thermal energies. Furthermore, the fraction of the solid surface area associated with given values of h_r and f that will contribute to colloid detachment from the primary minimum increases with increasing pH and a reduction in IS (Fig. 4). These findings are consistent with a number of column studies that have indicated reversible primary minimum retention with alteration of solution chemistry (e.g. Bradford et al., 2015a, b; Torkzaban et al., 2013).

4. Conclusions

This study elucidated the importance of including NSR into colloid interaction energy and microscale surface roughness into torque balance calculations to explain processes of colloid retention and release in porous media. In particular, we showed that NSR would reduce the depth of primary and secondary minima, the energy barrier to attachment in the primary minimum, and the energy barrier to detachment from the primary minimum. These findings suggest that NSR is expected to reduce colloid retention in secondary minima, and instead enhance colloid retention in primary minima. However, colloid retention in primary minima on locations containing nanoscale rough is expected to be weak and susceptible to removal via hydrodynamic shear and/or diffusion, especially when the solution IS and pH is reduced or increased, respectively. Consequently, only a fraction of the solid surfaces in porous media may contribute to colloid retention even under favorable chemical conditions. Contrary to NSR, microscale roughness was found to play a key role in enhancing colloid retention through reducing the lever arm associated with the applied hydrodynamic torque and increasing the lever arm for the resisting adhesive torque. Consequently, significant amounts of colloid retention are expected to occur in porous media when the applied hydrodynamic and resisting adhesive torques are not altered with time such as in column studies. In contrast, little colloid retention is expected in this same porous media when the direction and magnitude of the lever arms are constantly changing such as in batch systems. This information is needed to better understand and predict colloid interactions, retention, and release in natural and engineering applications.

Acknowledgment

This research was supported by the Gas Industry Social and Environmental Research Alliance (GISERA), a collaborative vehicle established by CSIRO and Australia Pacific LNG to undertake publicly-reported research addressing the socio-economic and

environmental impacts of Australia's natural gas industries. We would also like to acknowledge the help of Svantje Treumann in conducting some of the experiments.

Appendix A. Supplementary data

Supplementary data related to this article can be found at http://dx.doi.org/10.1016/j.watres.2015.10.022.

The supporting material contains details pertaining to: (i) properties of colloids and porous medium (S1); (ii) extended-DLVO calculations (S2); (iii) batch experiments (S3); (iv) SEM imaging (S4); and (v) torque balance calculations for batch experiments (S5). Table S1 contains zeta potential and interaction energy parameters for homogeneous colloids and sands. Table S2 presents detailed mass balance information for the column experiments. Table S3 presents calculated values of S_{max} and S_f in the batch experiments. Fig. S1 presents representative SEM images of colloid retention following the batch experiments.

References

Argent, J., Torkzaban, S., Hubbard, S., Le, H., Amirianshoja, T., Haghighi, M., 2015. Visualization of micro-particle retention on a heterogeneous surface using micro-models: Influence of nanoscale surface roughness. Transp. Porous Media 1–15.

Bendersky, M., Davis, J.M., 2011. DLVO interaction of colloidal particles with topographically and chemically heterogeneous surfaces. J. Colloid Interface Sci. 353 (1), 87–97.

Bergendahl, J., Grasso, D., 1999. Prediction of colloid detachment in a model porous media: Thermodynamics. AIChE J. 45, 475–484.

Bhattacharjee, S., Ko, C.-H., Elimelech, M., 1998. DLVO interaction between rough surfaces. Langmuir 14, 3365–3375.

Bowen, W.R., Doneva, T.A., 2000. Atomic force microscopy studies of membranes: effect of surface roughness on double-layer interactions and particle adhesion. J. Colloid Interface Sci. 229, 544–549.

Bradford, S.A., Torkzaban, S., Kim, H., Simunek, J., 2012. Modeling colloid and microorganism transport and release with transients in solution ionic strength. Water Resour. Res. 48, 9. http://dx.doi.org/10.1029/2012WR012468.

Bradford, S.A., Torkzaban, S., 2012. Colloid adhesive parameters for chemically heterogeneous porous media. Langmuir 28 (38), 13643–13651.

Bradford, S.A., Torkzaban, S., Shapiro, A., 2013. A theoretical analysis of colloid attachment and straining in chemically heterogeneous porous media. Langmuir 29, 6944–6952.

Bradford, S.A., Torkzaban, S., 2013. Colloid interaction energies for physically and chemically heterogeneous porous media. Langmuir 29 (11), 3668–3676.

Bradford, S.A., Wang, Y., Kim, H., Torkzaban, S., Šimůnek, J., 2014. Modeling microorganism transport and survival in the subsurface. J. Environ. Qual. 43 (2), 421–440.

Bradford, S.A., Torkzaban, S., Leij, F., Simunek, J., 2015a. Equilibrium and kinetic models for colloid release under transient solution chemistry conditions. J. Contam. Hydrol. 181, 141–152. http://dx.doi.org/10.1016/j.jconhyd.2015.04.003.

Bradford, S.A., Wang, Y., Torkzaban, S., Šimůnek, J., 2015b. Modeling the release of E. coli D21g with transients in water content. Water Resour. Res. 51, 3303–3316. http://dx.doi.org/10.1002/2014WR016566.

Chen, G., Bedi, R.S., Yan, Y.S., Walker, S.L., 2010. Initial colloid deposition on bare and zeolite-coated stainless steel and aluminum: Influence of surface roughness. Langmuir 26, 12605–12613.

Chrysikopoulos, C.V., Syngouna, V.I., 2014. Effect of gravity on colloid transport through water-saturated columns packed with glass beads: modeling and experiments. Environ. Sci. Technol. 48, 6805–6813.

Darbha, G.K., Fischer, C., Michler, A., Luetzenkirchen, J., Schafer, T., Heberling, F., Schild, D., 2012. Deposition of latex colloids at rough mineral surfaces: an analogue study using nanopatterned surfaces. Langmuir 28, 6606–6617.

Derjaguin, B.V., Landau, L.D., 1941. Theory of the stability of strongly charged lyophobic sols and of the adhesion of strongly charged particles in solutions of electrolytes. Acta Physicochim. U.S.S.R 14, 733–762.

Elimelech, M., O'Melia, C.R., 1990. Effect of particle size on collision efficiency in the deposition of Brownian particles with electrostatic energy barriers. Langmuir 443 (6), 1153–1163.

Emelko, M.B., 2003. Removal of viable and inactivated CryptosporidiumOocysts by dual- and Tri-Media filtration. Water Res. 37 (12), 2998–3008.

Foppen, J.W.A., Schijven, J.F., 2006. Evaluation of data from the literature on the transport and survival of Escherichia coli and thermotolerant coliforms in aquifers under saturated conditions. Water Res. 40, 401–426.

Gregory, J., 1981. Approximate expression for retarded van der Waals interaction. J. Colloid Interface Sci. 83, 138–145.

Henry, C., Minier, J.-P., Lefevre, G., Hurisse, O., 2011. Numerical study on the deposition rate of hematite particle on polypropylene walls: role of surface roughness. Langmuir 27, 3603–4612.

Hoek, E.M.V., Agarwal, G.K., 2006. Extended DLVO interactions between spherical particles and rough surfaces. J. Colloid Interface Sci. 298, 50–58.

Hogg, R., Healy, T.W., Fuerstenau, D.W., 1966. Mutual coagulation of colloidal dispersions. Trans. Faraday Soc. 62, 1638–1651.

Huang, X., Bhattacharjee, S., Hoek, E.M.V., 2010. Is surface roughness a "scapegoat" or a primary factor when defining particle-substrate interactions? Langmuir 26, 2528–2537.

Jaisi, D.P., Elimelech, M., 2009. Single-walled carbon nanotubes exhibit limited trans-port in soil columns. Environ. Sci. Technol. 43, 9161–9166.

Johnson, P.R., Elimelech, M., 1995. Dynamics of colloid deposition in porous media: blocking based on random sequential adsorption. Langmuir 11, 801–812.

Katainen, J., Paajanen, M., Ahtola, E., Pore, V., Lahtinen, J., 2006. Adhesion as an interplay between particle size and surface roughness. J. Colloid Interface Sci. 304, 524–529.

Khilar, K., Fogler, S., 1998. Migration of Fines in Porous Media. Kluwer Academic Publishers, Dordrecht.

Knappett, P., Emelko, M.B., Zhuang, J., McKay, L., 2008. Transport and retention of MS-2 bacteriophage and microspheres in saturated porous media: impact of ionic strength and grain size. Water Res. 42 (16), 4368–4378.

Konopinski, D., Hudziak, S., Morgan, R., Bull, P., Kenyon, A., 2012. Investigation of quartz grain surface textures by atomic force microscopy for forensic analysis. Forensic Sci. Int. 223, 245–255.

Kuznar, Z.A., Elimelech, M., 2007. Direct microscopic observation of particle deposition in porous media: role of the secondary energy minimum. Colloids Surf. A Physicochem. Eng. Aspects 294 (1–3), 156–162.

Liu, Y., Janjaroen, D., Kuhlenschmidt, M.S., Kuhlenschmidt, T.B., Nguyen, T.H., 2009. Deposition of Cryptosporidium parvum oocysts on natural organic matter surfaces: microscopic evidence for secondary minimum deposition in a radial stagnation point flow cell. Langmuir 25, 1594–1605.

Magal, E., Weisbrod, N., Yechieli, Y., Walker, S.L., Yakirevich, A., 2011. Colloid transport in porous media: Impact of hyper-saline solutions. Water Res. 45, 3521–3532.

Morales, V.L., Gao, B., Steenhuis, T.S., 2009. Grain surface-roughness effects on colloid retention in the vadose zone. Vadose Zone J. 8 (1), 11–20.

Ruckenstein, E., Prieve, D.C., 1976. Adsorption and desorption of particles and their chromatographic separation. AIChE J. 22, 276–285.

Ryan, J.N., Elimelech, M., 1996. Colloid mobilization and transport in groundwater. Colloids Surf. A 107, 1–56.

Ryan, J.N., Gschwend, P.M., 1994. Effects of ionic strength and flow rate on colloid release: relating kinetics to intersurface potential energy. J. Colloid Interface Sci. 164 (1), 21–34.

Sasidharan, S., Torkzaban, S., Bradford, S.A., Dillon, P.J., Cook, P.G., 2014. Coupled effects of hydrodynamic and solution chemistry on long-term nanoparticle transport and deposition in saturated porous media. Colloids Surf. A Physicochem. Eng. Aspects 457, 169–179.

Shang, W., Morales, V.L., Zhang, W., Stoof, C.R., Gao, B., Schatz, A.L., Zhang, Y., Steenhuis, T.S., 2013. Quantification of colloid retention and release by straining and energy minima in variably saturated porous media. Environ. Sci. Technol. 47, 8256–8264.

Shellenberger, K., Logan, B.E., 2002. Effect of molecular scale roughness of glass beads on colloidal and bacterial deposition. Environ. Sci. Technol. 36, 184–189.

Shen, C., Li, B., Wang, C., Huang, Y., Jin, Y., 2011. Surface roughness effect on deposition of nano- and micro-sized colloids in saturated columns at different solution ionic strengths. Vadose Zone J. 10, 1071–1081.

Shen, C., Lazouskaya, V., Zhang, H., Li, B., Jin, Y., Huang, Y., 2013. Influence of surface chemical heterogeneity on attachment and detachment of microparticles. Colloids Surf. A 433, 14–29.

Shen, C., Wang, L.-P., Li, B., Huang, Y., Jin, Y., 2012. Role of surface roughness in chemical detachment of colloids deposited at primary energy minima. Vadose Zone J. 11 http://dx.doi.org/10.2136/vzj2011.0057.

Simoni, S.F., Harms, H., Bosma, T.N.P., Zehnder, A.J.B., 1998. Population heterogeneity affects transport of bacteria through sand columns at low flow rates. Environ. Sci. Technol. 32, 2100–2105.

Suresh, L., Walz, J.Y., 1996. Effect of surface roughness on the interaction energy between a colloidal sphere and a flat plate. J. Colloid Interface Sci. 183 (1), 199–213.

Syngouna, V.I., Chrysikopoulos, C.V., 2011. Transport of biocolloids in water saturated columns packed with sand: effect of grain size and pore water velocity. J. Contam. Hydrol. 126, 301–314.

Tong, M., Ma, H., Johnson, W.P., 2008. Funnelling of flow into grain to-grain contacts drives colloid-colloid aggregation in the presence of an energy barrier. Environ. Sci. Technol. 42, 2826–2832.

Torkzaban, S., Tazehkand, S.S., Walker, S.L., Bradford, S.A., 2008. Transport and fate of bacteria in porous media: coupled effects of chemical conditions and pore space geometry. Water Resour. Res. 44 http://dx.doi.org/10.1029/2007WR006541.

Torkzaban, S., Kim, H.N., Simunek, J., Bradford, S.A., 2010. Hysteresis of colloid retention and release in saturated porous media during transients in solution chemistry. Environ. Sci. Technol. 44, 1662–1669.

Torkzaban, S., Bradford, S.A., Vanderzalm, J.L., Patterson, B.M., Harris, B., Prommer, H., 2015. Colloid release and clogging in porous media: effects of solution ionic strength and flow velocity. J. Contam. Hydrol. 181, 161–171. http://dx.doi.org/10.1016/j.jconhyd.2015.06.005.

Torkzaban, S., Bradford, S.A., Wan, J., Tukunaga, T., Masoudih, A., 2013. Release of quantum dot nanoparticles in porous media: role of cation exchange and aging time. Environ. Sci. Technol. 47, 11528–11536.
Tosco, T., Tiraferri, A., Sethi, R., 2009. Ionic strength dependent transport of microparticles in saturated porous media: modeling mobilization and immobilization phenomena under transient chemical conditions. Environ. Sci. Technol. 43, 4425–4431.
Treumann, S., Torkzaban, S., Bradford, S.A., Visalakshan, R.M., Page, D., 2014. An explanation for differences in the process of colloid adsorption in batch and column studies. J. Contam. Hydrol. 164 (0), 219–229.
Tufenkji, N., Miller, G.F., Ryan, J.N., Harvey, R.W., Elimelech, M., 2004. Transport of *Cryptosporidium* oocysts in porous media: role of straining and physicochemical filtration. Environ. Sci. Technol. 38, 5932–5938.
Tufenkji, N., Elimelech, M., 2005. Breakdown of colloid filtration theory: role of the secondary energy minimum and surface charge heterogeneities. Langmuir 21, 841–852.
van Oss, C.J., 1994. Interfacial Forces in Aqueous Media. Marcel Dekker (New York).
Verwey, E.J.W., Overbeek, J.ThG., 1948. Theory of the Stability of Lyophobic Colloids. Elsevier, Amsterdam.